Inorg. Chem. **2002**, *41*, 5440–5452

Copper–Bispidine Coordination Chemistry: Syntheses, Structures, Solution Properties, and Oxygenation Reactivity

Heidi Börzel,[†] Peter Comba,*[,†] Karl S. Hagen,[‡] Marion Kerscher,[†] Hans Pritzkow,[†] Markus Schatz,[§] Siegfried Schindler,[§] and Olaf Walter[||]

Anorganisch-Chemisches Institut der Universität Heidelberg, Im Neuenheimer Feld 270, D-69120 Heidelberg, Germany, Department of Chemistry, Emory University, 1515 Pierce Drive, Atlanta, Georgia 30322, Institut für Anorganische Chemie, Universität Erlangen-Nürnberg, Egerlandstrasse 1, D-91058 Erlangen, Germany, and Forschungszentrum Karlsruhe GmbH, ITC-CPV, Postfach 3640, 76021 Karlsruhe, Germany

Received October 29, 2001

Copper(I) and copper(II) complexes of two mononucleating and four dinucleating tetradentate ligands with a bispidine backbone (2,4-substituted (2-pyridyl or 4-methyl-2-pyridyl) 3,7-diazabicyclo[3.3.1]nonanone) have been prepared and analyzed structurally, spectroscopically, and electrochemically. The structures of the copper chromophores are square pyramidal, except for two copper(I) compounds which are four-coordinate with one noncoordinated pyridine. The other copper(I) structures have the two pyridine donors, the co-ligand ($NCCH_3$), and one of the tertiary amines (N3) in-plane with the copper center and the other amine (N7) coordinated axially (Cu–N3 > Cu–N7, approximately 2.25 Å vs 2.20 Å). The copper(II) compounds with pyridine donors have a similar structure, but the axial amine has a weaker bond to the copper(II) center (Cu–N3 < Cu–N7, approximately 2.03 Å vs 2.30 Å). The structures with methylated pyridine donors are also square pyramidal with the co-ligands (Cl^- or $NCCH_3$) in-plane. With $NCCH_3$ the same structural type as for the other copper(II) complexes is observed, and with the bulkier Cl^- the co-ligand is trans to N7, leading to a square pyramidal structure with the pyridine donors rotated out of the basal plane and only a small difference between axial and in-plane amines (2.15, 2.12 Å). These structural differences, enforced by the rigid bispidine backbone, lead to large variations in spectroscopic and electrochemical properties and reactivities. Oxygenation of the copper(I) complexes with pyridine-substituted bispidine ligands leads to relatively stable μ-peroxo–dicopper(II) complexes; with a preorganization of the dicopper chromophores, by linking the two donor sets, these peroxo compounds are stable at room temperature for up to 1 h. The stabilization of the peroxo complexes is to a large extent attributed to the square pyramidal coordination geometry with the substrate bound in the basal plane, a structural motif enforced by the rigid bispidine backbone. The stabilities and structural properties are also seen to correlate with the spectroscopic (UV–vis and Raman) and electrochemical properties.

Introduction

Activation of molecular dioxygen plays an important role in biological and industrial processes.[1−4] Nature uses metalloenzymes to overcome the inactivity of triplet dioxygen; activation occurs primarily via electron transfer from the metal centers to the dioxygen molecule, and redox active metal ions such as iron, copper, and manganese play an important role in active sites of dioxygen activating enzymes.[5,6] The binding mode of oxygen in copper enzymes for dioxygen transport and activation has been analyzed in a number of structural, spectroscopic, and mechanistic studies (see, e.g., refs 2−4 and 7−12).

* Author to whom correspondence should be addressed. E-mail: comba@akcomba.oci.uni-heidelberg.de. Fax: +49 6221 54 6617.
[†] Universität Heidelberg.
[‡] Emory University.
[§] Universität Erlangen-Nürnberg.
[||] Forschungszentrum Karlsruhe GmbH.

(1) Reedijk, J.; Bouwman, E. *Bioinorganic Catalysis*, 2nd ed.; Marcel Dekker: New York, 1999.
(2) Liang, H.-C.; Dahan, M.; Karlin, K. D. *Curr. Opin. Chem. Biol.* **1999**, *3* (2), 168.
(3) Blackman, A. G.; Tolman, W. B. In *Structure & Bonding*; Meunier, B., Ed.; Springer: Berlin, 2000; Vol. 97, p 179.
(4) Schindler, S. *Eur. J. Inorg. Chem.* **2000**, 2311.
(5) Lippard, S. J.; Berg, J. M. *Principles of bioinorganic chemistry*, 3rd ed.; University Science Books: Mill Valley, 1994.
(6) Kaim, W.; Schwederski, B. *Bioanorganische Chemie*, 2nd ed.; B. G. Teuber: Stuttgart, 1995.
(7) Tyeklar, Z.; Karlin, K. D. *Acc. Chem. Res.* **1989**, *22*, 241.

10.1021/ic011114u CCC: $22.00
Published on Web 09/26/2002

Chart 1

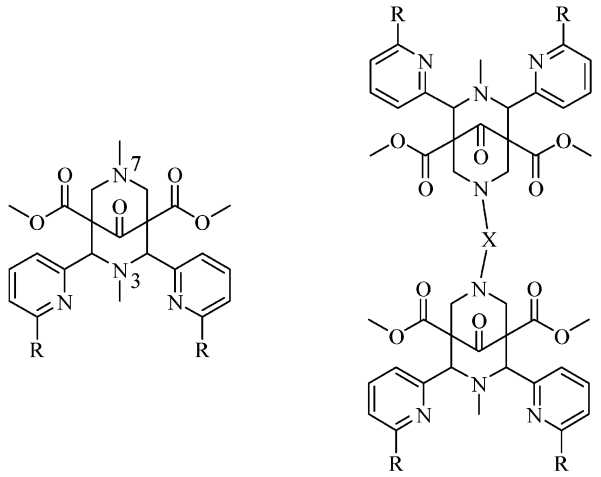

L^1	R = H	L^2	X = ethyl	R = H
Me-L^1	R = CH_3	Me-L^2	X = ethyl	R = CH_3
		L^3	X = propyl	R = H
		L^4	X = meta-xylyl	R = H

Hemocyanin, the dioxygen transport enzyme found in mollusks and anthropods, contains a dicopper center in its active site; dioxygen is bound reversibly in a μ-η^2-η^2 fashion. In model systems, several binding modes have been observed, and some of these are believed to be important intermediates in the enzymatic processes: peroxide may bridge two copper centers in an end-on trans-μ-1,2 mode[7,8,13,14] (*cis*-μ-1,2-peroxo compounds are uncommon in copper chemistry but have been observed with iron and cobalt[15,16]); μ-η^2-η^2 peroxo-bridged dicopper(II) species[17,18] have also been described, as well as bis-μ-oxo dicopper(III) isomers,[19,20] and the latter two forms have been found to be in equilibrium in various examples;[21−24] tetranuclear copper(II) compounds with μ^4-bound dioxygen have also been structurally characterized.[25−27] Mononuclear superoxo complexes have been suggested as intermediates in the formation of the peroxo complexes, generated by one-electron instead of two-electron transfer occurring from the metal center to dioxygen; superoxide has been found to coordinate in either a side-on or end-on fashion.[28−30]

Oxygenation of copper(I) complexes with bispidine-type ligands leads to unusually stable end-on μ-peroxo-dicopper(II) compounds (for the basic ligand structure of the tetradentate bispidine ligands, see Chart 1, 2,4-substituted bispidones, 3,7-diazabicyclo[3.3.1]nonanone).[31,32] Bispidine-type ligands are very rigid and enforce for pentacoordinate complexes a square pyramidal structure (octahedral for hexacoordinate compounds), with the substrate coordinated in an equatorial position.[31−36] The rigid bispidine backbone is particularly well suited for the Jahn−Teller labile

(8) Karlin, K. D.; Kaderli, S.; Zuberbühler, A. D. *Acc. Chem. Res.* **1997**, *30*, 139.
(9) Kitajima, N.; Moro-oka, Y. *Chem. Rev.* **1994**, *94*, 737.
(10) Lee, D.-H.; Wei, N.; Murthy, N. N.; Tyeklar, Z.; Karlin, K. D.; Kaderli, S.; Jung, B.; Zuberbühler, A. D. *J. Am. Chem. Soc.* **1995**, *117*, 12498.
(11) Mahapatra, S.; Kaderli, S.; Llobet, A.; Neuhold, Y.-M.; Palanche, T.; Halfen, J. A.; Young, J., V. G.; Kaden, T. A.; Que, J., L.; Zuberbuehler, A. D.; Tolman, W. B. *Inorg. Chem.* **1997**, *36*, 6343.
(12) Asato, E.; Hashimoto, S.; Matsumoto, N.; Kida, S. *J. Chem. Soc., Dalton Trans.* **1990**, 1741.
(13) Tyeklar, Z.; Jacobson, R. R.; Wei, N.; Murthy, N. N.; Zubieta, J.; Karlin, K. D. *J. Am. Chem. Soc.* **1993**, *115*, 2677.
(14) He, C.; DuBois, J. L.; Hedman, B.; Hodgson, K. O.; Lippard, S. J. *Angew. Chem., Int. Ed.* **2001**, *40*, 1484.
(15) Niederhoeffer, E. C.; Trimmens, J. H.; Martell, A. E. *Chem. Rev.* **1984**, *84*, 137.
(16) Hummel, H.; Mekamouche, Y.; Duboc-Toia, C.; Ho, R. Y. N.; Que, J. L.; Schünemann, V.; Thomas, F.; Trautwein, A. X.; Lebrun, C.; Fontecave, M.; Ménage, S. *Angew. Chem.* **2002**, *114*, 639.
(17) Kitajima, N.; Fujisawa, K.; Fujimoto, C.; Moro-Oka, Y.; Hashimoto, S.; Kitagawa, T.; Toriumi, K.; Tatsumi, K.; Nakamura, A. *J. Am. Chem. Soc.* **1992**, *114*, 1277.
(18) Kodera, M.; Katayama, K.; Tachi, Y.; Kano, K.; Hirota, S.; Fujinami, S.; Suzuki, M. *J. Am. Chem. Soc.* **1999**, *121*, 11006.
(19) Tolman, W. B. *Acc. Chem. Res.* **1997**, *30*, 227.
(20) Straub, B.; Rominger, F.; Hofmann, P. *Chem. Commun.* **2000**, *17*, 1611.
(21) Cahoy, J.; Holland, P.; Tolman, W. B. *Inorg. Chem.* **1999**, *38*, 2161.
(22) Obias, H. V.; Lin, Y.; Murthy, N. N.; Pidcock, E.; Solomon, E. I.; Ralle, M.; Blackburn, N. J.; Neuhold, Y.-M.; Zuberbühler, A. D.; Karlin, K. D. *J. Am. Chem. Soc.* **1998**, *120*, 12960.
(23) Mahadevan, V.; Henson, M. J.; Solomon, E. I.; Stack, T. D. P. *J. Am. Chem. Soc.* **2000**, *122*, 10249.
(24) Liang, H.-C.; Zhang, C. X.; Henson, M. J.; Sommer, R. D.; Hatwell, K. R.; Kaderli, S.; Zuberbühler, A. D.; Rheingold, A. L.; Solomon, E. I.; Karlin, K. D. *J. Am. Chem. Soc.* **2002**, *124*, 4170.
(25) Reim, J.; Werner, R.; Haase, W.; Krebs, B. *Chem. Eur. J.* **1998**, *4*, 289.
(26) Neyhart, G. A.; Marshall, J. L.; Dressick, B.; Sullivan, B. P.; Watkins, P. A.; Meyer, T. J. *J. Chem. Soc., Chem. Commun.* **1982**, 915.
(27) Meyer, F.; Pritzkow, H. *Angew Chem., Int. Ed.* **2000**, *39*, 2112.
(28) Fujisawa, K.; Tanaka, M.; Moro-oka, Y.; Kitajima, N. *J. Am. Chem. Soc.* **1994**, *116*, 12079.
(29) Tahir, M. M.; Karlin, K. D. *J. Am. Chem. Soc.* **1992**, *114*, 7599.
(30) Wei, N.; Murthy, N. N.; Chen, Q.; Zubieta, J.; Karlin, K. D. *Inorg. Chem.* **1994**, *33*, 1953.
(31) Börzel, H.; Comba, P.; Hagen, K. S.; Katsichtis, C.; Pritzkow, H. *Chem. Eur. J.* **2000**, *6*, 914.
(32) Börzel, H.; Comba, P.; Katsichtis, C.; Kiefer, W.; Lienke, A.; Nagel, V.; Pritzkow, H. *Chem. Eur. J.* **1999**, *5*, 1716.
(33) Comba, P.; Nuber, B.; Ramlow, A. *J. Chem. Soc., Dalton Trans.* **1997**, 347.
(34) Comba, P.; Kanellakopulos, B.; Katsichtis, C.; Lienke, A.; Pritzkow, H.; Rominger, F. *J. Chem. Soc., Dalton Trans.* **1998**, 3997.
(35) Comba, P.; Lienke, A. *Inorg. Chem.* **2001**, *40*, 5206.
(36) Börzel, H.; Comba, P.; Pritzkow, H. *Chem. Commun.* **2001**, 97.

Scheme 1[a]

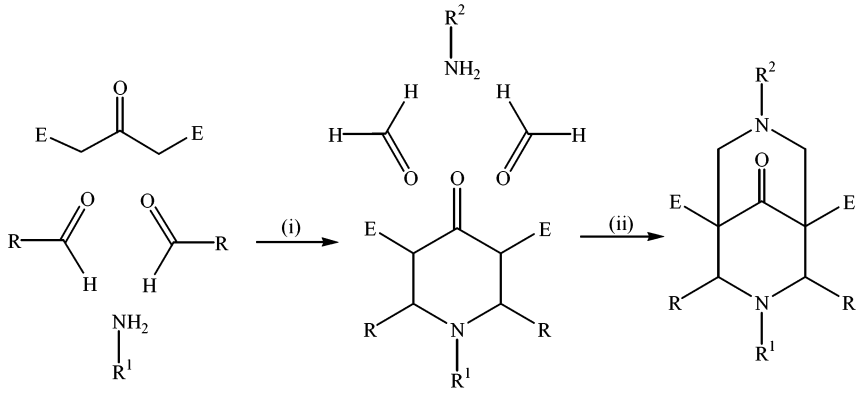

[a] (i) MeOH, 0 °C; (ii) EtOH (L^1, Me-L^1), MeOH (L^4), THF (L^2, Me-L^2, L^3), Δ (10 min to 1 h).

copper(II) center.[31,32,35−38] Dinucleating ligands are known to lead to an enhanced stability of dicopper(II) peroxo compounds,[18,39−41] and the oxygenation product of L^2 coordinated to copper(I) (Chart 1) is one of the most stable end-on μ-peroxo−dicopper(II) complexes known so far.[32] Note, that, due to strain, peroxo complexes based on dinucleating ligands are generally enthalpically less stable than those based on mononucleating ligands.[8,10,22] We present here a detailed study of the structural properties and reactivities of a series of copper(I) and copper(II) complexes with bispidine-type dinucleating ligands with various spacer groups.

Results and Discussion

Ligand Syntheses. All ligands were prepared by a two-step Mannich reaction, with the methyl ester of acetone dicarboxylate, pyridine aldehyde, and methylamine in THF or MeOH, leading to the piperidone precursors. The piperidones were then reacted with an amine and formaldehyde to give the bispidone compounds (see Scheme 1). They were isolated and separated from byproducts by evaporation of the solvent and addition of MeOH or EtOH, in which the ligands are only sparingly soluble. The series of ligands (see Chart 1) was obtained by varying the amine component in the second reaction step; the aldehyde component can also be used to modify the ligand structure and donor set.[31,42,43] The yields of the ligands described here range, dependent on the amine used, from 3% to 88%; usually they are around 70%.

Syntheses of the Copper Complexes. Copper(I) Compounds. The copper(I) compounds were isolated by mixing a suspension of the ligand and the corresponding copper(I) salt in acetonitrile and an argon atmosphere, followed by ether diffusion into the solution at ambient temperature. When halogenated solvents, such as dichloromethane, were used or when the copper(I) complexes were reacted with halogenated substrates, oxidation to the corresponding copper(II) chloro compound took place, a reaction well-known for other copper(I) compounds.[10,13,30,44] Acetone, as a noncoordinating solvent, allowed the isolation of the copper(I) compounds of L^1 and L^3; the [Cu(L^2)] complex reacted in a disproportionation reaction to the corresponding copper(II) compound and copper metal. However, when [Cu(CH_3CN)$_4$]SbF_6 as the copper(I) source and very dilute solutions were used, a dicopper(I) compound of $L^{2'}$ (in which L^2 had been modified in the complexation reaction, see below) could be isolated.

Copper(II) Compounds. These were prepared and isolated by mixing the ligands and a copper(II) salt in acetonitrile, followed by ether diffusion into the solution. When copper(II) salts with potentially coordinating counterions, such as Cl^-, NO_3^-, or CH_3COO^-, were used, crystalline products were obtained. With noncoordinating counterions, such as ClO_4^- and BF_4^-, crystallization of the copper(II) products was achieved by addition of tetrachlorocatechol, which decreases the solubility of the copper(II) complexes; note that isolation of the corresponding catecholate compounds requires the presence of base.[36] The copper(II) compounds have a blue to turquoise color, dependent on the counterion and the ligand used, and are soluble in water, methanol, and acetonitrile.

Solid-State Structures. Copper(I) Compounds. ORTEP[45] drawings of the crystallographically determined structures of the molecular cations of [Cu_2(L^3)($NCCH_3$)$_2$](PF_6)$_2$ and [Cu_2($L^{2'}$)($NCCH_3$)$_2$](SbF_6)$_2$ ($L^{2'}$ is a derivative of L^2 with inverted configuration at C2, see Chart 1) are shown in Figure 1; selected structural parameters are shown in Table 1 (also presented in Figure 1 and Table 1 are the structural data of [Cu(L^1)($NCCH_3$)]X (X = OTf^-, BF_4^-), which have been reported previously[31]).

Two isomers have been observed for [Cu(L^1)($NCCH_3$)]$^+$, a yellow four-coordinate form (distorted tetrahedral) and a red-orange five-coordinate compound (distorted square pyr-

(37) Comba, P.; Merz, M.; Pritzkow, H., in preparation.
(38) Comba, P.; Schiek, W. *Coord. Chem. Rev.*, accepted.
(39) Comba, P.; Hilfenhaus, P.; Karlin, K. D. *Inorg. Chem.* **1997**, *36*, 2309.
(40) Karlin, K. D.; Lee, D. H.; Kaderli, S.; Zuberbühler, A. D. *Chem. Commun.* **1997**, 475.
(41) Bol, J. E.; Driessen, W. L.; Ho, R. Y. N.; Maase, B.; Que, L., Jr.; Reedijk, J. *Angew. Chem., Int. Ed. Engl.* **1997**, *36*, 998.
(42) Comba, P.; Kerscher, M.; Merz, M. Publications in preparation.
(43) Börzel, H.; Comba, P.; Hagen, K. S.; Merz, M.; Lampeka, Y. D.; Lienke, A.; Linti, G.; Pritzkow, H.; Tsymbal, L. V. *Inorg. Chim. Acta* **2002**, *337*, 408.
(44) Becker, M.; Heinemann, F. W.; Schindler, S. *Chem. Eur. J.* **1999**, *5*, 3124.
(45) Johnson, C. K. *ORTEP, A Thermal Ellipsoid Plotting Program*; Oak National Laboratories: Oak Ridge, TN, 1965.

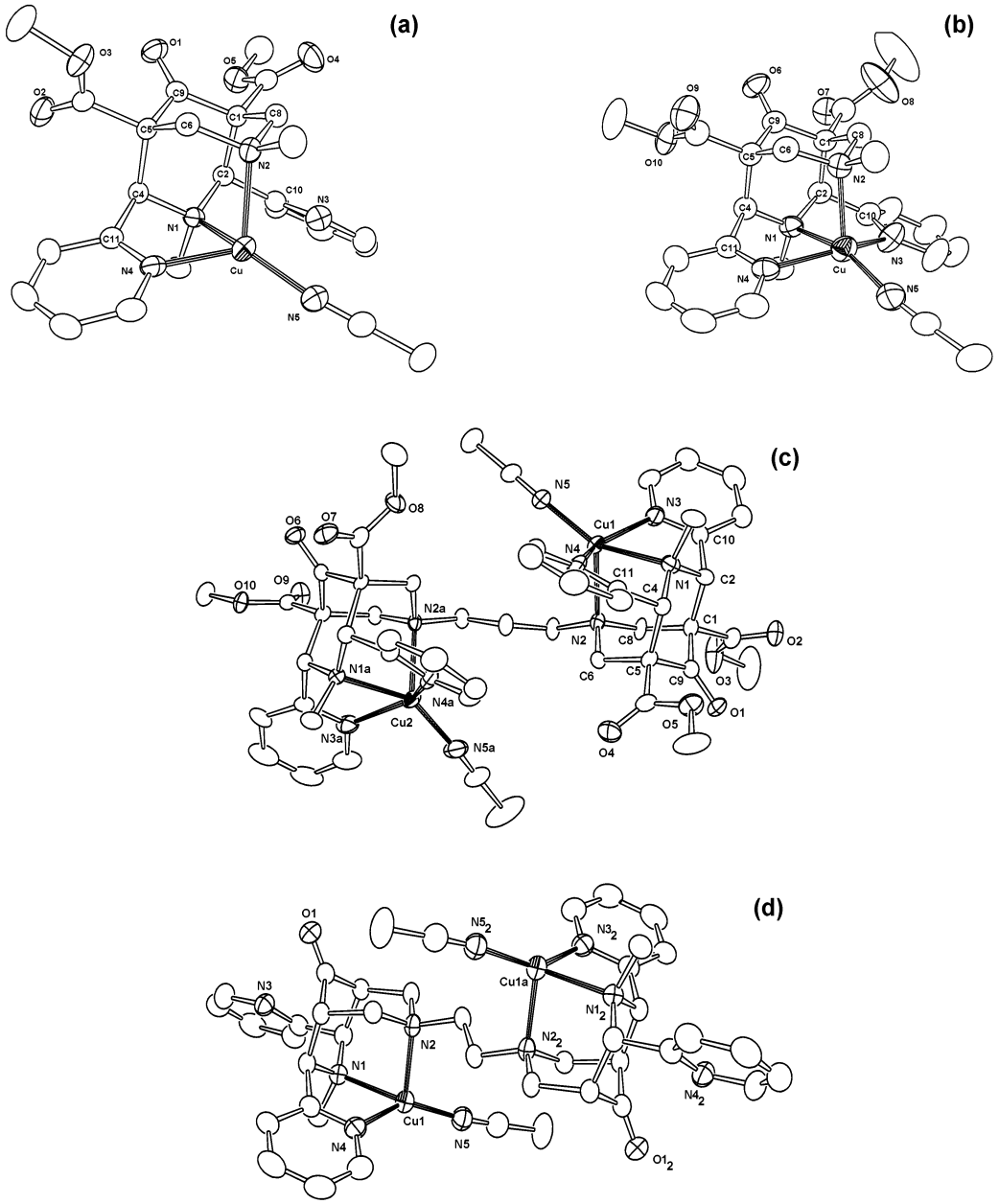

Figure 1. Cationic portions of the X-ray crystal structures of the Cu(I) complexes $[Cu(L^1)NCCH_3]X$ [(a) X = BF_4^-, (b) X = $CF_3SO_3^-$], (c) $[Cu_2(L^3)(NCCH_3)_2](PF_6)_2$, and (d) $[Cu_2(L^{2\prime})(NCCH_3)_2](SbF_6)_2$.

amidal).[31] The two copper(I) centers of the red-orange $[Cu_2(L^3)(NCCH_3)_2]^{2+}$ cation are five-coordinate, and those of $[Cu_2(L^{2\prime})(NCCH_3)_2]^{2+}$ are four-coordinate, because the two dangling pyridine groups cannot coordinate to the copper centers, due to the inversion at the C2 atoms. The mechanism of the epimerization, which occurred during the complexation reaction (this also emerges from ^{1}H NMR spectra when mixing L^2 and the copper(I) salt in acetone-d_6), is unclear, and a similar reaction has not been observed so far for any other bispidine ligand or with any other metal ion. In the two dinuclear complexes the two chromophores are rotated away from each other, and coordination of a bridging substrate (e.g., O_2) would require the alkyl bridges to rearrange.

In contrast to many other structurally characterized metal complexes of the bispidine type ligands shown in Chart 1,[31−34,36,37,43] the copper(I) structures do not show the same geometry as copper(II) (see below), which has a short Cu−N3 and a long Cu−N7 bond (note that the crystallographic numbering used in the tables and figures is different from the IUPAC numbering, see Chart 1).[47] The structural studies indicate that the tight and rigid bispidine ligand cavity is not as well suited for copper(I) as for copper(II) (see Table 1; this also emerges from electrochemistry, see below): while the ligand is relatively undistorted (see N···N distances, e.g.), there are large distortions in the copper chromophores,[31] and significant structural differences occur in the various geometries.

Copper(II) Compounds. ORTEP[45] plots of the crystallographically determined structures of the molecular cations

(46) Comba, P.; Kerscher, M.; Merz, M.; Müller, V.; Pritzkow, H.; Remenyi, R.; Schiek, W.; Xiong, Y. *Chem. Eur. J.*, accepted.
(47) Comba, P.; Schiek, W., in preparation.

Table 1. Structural Parameters[a] of the Copper(I) Compounds (a) $[Cu(L^1)(NCCH_3)]BF_4$, (b) $[Cu(L^1)(NCCH_3)]CF_3SO_3$, (c) $[Cu_2(L^3)(NCCH_3)_2](PF_6)_2$, and (d) $[Cu_2(L^{2\prime})(NCCH_3)_2](SbF_6)_2$

	a	b	c	d
Cu−N1	2.24	2.20	2.23/2.20	2.21
Cu−N2	2.16	2.16	2.18/2.20	2.19
Cu−N3	2.38	3.12	2.25/2.49	2.01
Cu−N4	2.25	2.07	2.34/2.21	
Cu−N5	1.98	1.87	1.93/1.91	1.86
N1−N2	2.95	2.91	2.95/2.95	2.93
N3−N4	4.41	4.95	4.37/4.50	5.36
Cu1···Cu2			6.408	6.04
C1−C2−C10−N3	83.5	64.6	83.9/80.1	97.4
C5−C4−C11−N4	−85.5	−82.7	−81.6/−84.9	52.9
N1−Cu−N2	84.07	83.77	83.96/84.05	83.38
N1−Cu−N3	72.73	65.74	74.10/72.03	80.73
N1−Cu−N4	75.11	79.58	73.21/76.47	
N1−Cu−N5	149.33	134.18	151.56/150.42	129.72
N2−Cu−N3	95.33	85.13	97.65/94.64	100.84
N2−Cu−N4	94.43	99.80	93.80/94.50	
N2−Cu−N5	125.59	118.48	124.30/122.84	107.20
N3−Cu−N4	144.71	144.31	143.88/146.00	
N3−Cu−N5	94.58	76.28	102.17/92.03	140.04
N4−Cu−N5	106.02	128.39	99.25/110.01	

[a] Distances in Å, angles in deg.

of $\{[Cu(L^1)]_2SO_4\}(SO_4)$, $[Cu_2(L^2)(NCCH_3)_2](ClO_4)_4$, and $[Cu_2(L^3)(Cl)_2]Cl_2$ are shown in Figure 2; selected structural parameters are presented in Table 2 (also presented in Figure 2 and Table 2 are the structural data of $[Cu(L^1)(Cl)]Cl$, $[Cu(Me\text{-}L^1)(Cl)]Cl$, and $[Cu(Me\text{-}L^1)(NCCH_3)](BF_4)_2$, which have been reported previously;[31] the crystals of $\{[Cu(L^1)]_2SO_4\}(SO_4)$ were of poor quality, and only a small data set was available for refinement; the connectivity of the molecular cation was obtained unambiguously, but refinement of the structure was not possible; consequently, the structural parameters are not presented in Table 2).

The chromophores of the copper(II) structures of L^1-L^3 are square pyramidal with N3, the two pyridine donors, and the extra ligand in-plane with copper(II), and N7 at the apical position. This configuration is enforced by the bispidine ligand,[38,46] and DFT studies[35] indicate that, in this configuration, the cavity has a high degree of complementarity for copper(II) and, therefore, leads to very stable complexes. This is supported by the fact that the geometry of the ligand backbone is basically undistorted[35,38] and that all copper chromophores have close to identical geometric parameters. The bonds to the in-plane monodentate ligands are relatively short and indicate that substrates (e.g., O_2) might be strongly bound to the copper center.[32,35] The bond to the axial amine (N7) is generally approximately 0.2 Å longer than that to the equatorial amine (N3).

In complexes with methylated pyridine donors ($Me\text{-}L^1$) the equatorial position for substrate coordination is sterically crowded (see structures of $[Cu(Me\text{-}L^1)(Cl)]^+$ and $[Cu(Me\text{-}L^1)(NCCH_3)]^+$ [31]), and two different square pyramidal structures are observed; with bulkier substrates (Cl^-), a structure with a quenched Jahn−Teller distortion and a considerably less strongly bound substrate is obtained.[35,46] The bispidine units in the molecular cations of the dinuclear complexes $[Cu_2(L^2)(NCCH_3)_2]^{4+}$ and $[Cu_2(L^3)(Cl)_2]^{2+}$ are rotated away from each other, similar to those of the dicopper(I) compounds above, resulting in comparably long Cu···Cu distances of 7.044 and 7.597 Å, respectively.

With $CuSO_4$ and L^1 a sulfato-bridged dicopper(II) complex was isolated; one of the ketalized OH groups reacted with the solvent MeOH, used in the complexation reaction to form a methyl ether. The free in-plane coordination sites are occupied by sulfate oxygen atoms. These Cu−O bonds are relatively short (approximately 1.94 Å), but within the expected limits for sulfate-bridged dicopper(II) complexes (1.91−1.97 Å).[48]

Solution Properties of the Copper Compounds. ^{1}H NMR Spectroscopy of the Copper(I) Complexes. In an earlier publication the ^{1}H NMR spectra of $[Cu(L^1)(NCCH_3)]^+$ were reported to show broad, ill-defined signals at ambient temperature with sharp signals at low temperature; the spectra of $[Cu(Me\text{-}L^1)]^+$ (the absence of coordinated solvent molecules emerges from the elemental analysis and the absence of the corresponding ^{1}H NMR signals) were reported to have already sharp signals at ambient temperature.[31] The line broadening was attributed to a fast equilibrium between two structures, with L^1 coordinated as a tetradentate or as a tridentate ligand, i.e., with one pyridine donor switching on or off the copper(I) center. This was supported by structural studies, i.e., both isomers (tetradentate coordination mode, square pyramidal with an additional $NCCH_3$ donor; tridentate coordination mode, tetrahedral, additional $NCCH_3$ donor) were analyzed by X-ray studies (different salts, see above).[31] Also, this interpretation is similar to observations and their interpretation with the copper(I) complex of tmpa.[49] While a dynamic process, based on the structural observations, is likely to occur, this involves bond-breaking and bond-making, and the corresponding activation barriers might be appreciable but are unknown. More recent ^{1}H NMR studies indicate that the line broadening might also be due to fast electron self-exchange between the copper(I) form of $[Cu(L^1)(NCCH_3)]^+$ (pentacoordinate) and some impurity of the corresponding oxidized form.[50] This is supported by the observation that the reduced form of the complex with L^1 is much more sensitive toward oxidation than that with $Me\text{-}L^1$ (see below), and that computation of the inner-sphere reorganization barriers[51−53] leads to the expectation that the electron self-exchange in $[Cu(L^1)(NCCH_3)]^{2+/+}$ is fast, while that in $[Cu(Me\text{-}L^1)]^{2+/+}$ is by several orders of magnitude slower. Detailed studies of the electron self-exchange kinetics and their influence on the ^{1}H NMR line shapes of the bispidine copper(I) complexes will be reported elsewhere.[50]

While all other ^{1}H NMR spectra of the copper(I) complexes show the typical features of a highly symmetrical

(48) Koningsbruggen, J. V.; Gatteschi, D.; Graaff, R. A. G. D.; Haasnoot, J. G.; Reedijk, J.; Zanchini, C. *Inorg. Chem.* **1995**, *34*, 5175.
(49) Tyeklar, Z.; Jacobson, R. R.; Wei, N.; Murthy, N. N.; Zubieta, J.; Karlin, K. D. *J. Am. Chem. Soc.* **1993**, *115*, 2677.
(50) Comba, P.; Kerscher, M.; Roodt, A., work in progress.
(51) Comba, P.; Sickmüller, A. F. *Inorg. Chem.* **1997**, *36*, 4500.
(52) Comba, P.; Hambley, T. W. *Molecular Modeling of Inorganic Compounds. 2nd Edition with a Tutorial, based on MOMEClite*, 2nd ed.; Wiley-VCH: Weinheim, 2001.
(53) Xie, B.; Elder, T.; Wilson, L. J.; Stanbury, D. M. *Inorg. Chem.* **1999**, *38*, 12.

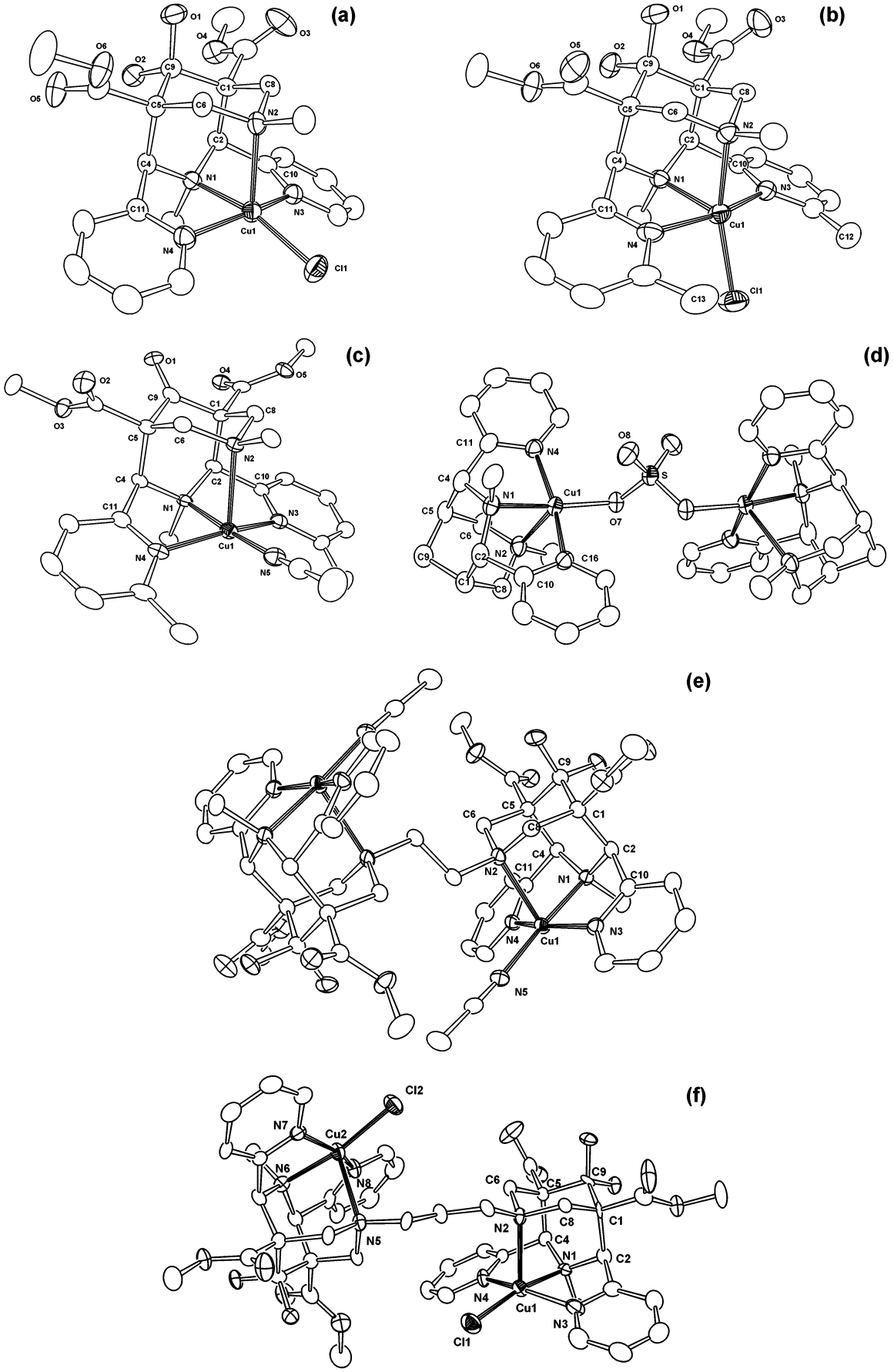

Figure 2. Cationic portions of the X-ray crystal structures of the Cu(II) complexes (a) $Cu(L^1)Cl]Cl$, (b) $[Cu(Me\text{-}L^1)Cl]Cl$, (c) $[Cu(Me\text{-}L^1)NCCH_3](BF_4)_2$, (d) $[Cu_2(L^1)_2SO_4]SO_4$, (e) $[Cu_2(L^2)(NCCH_3)_2](ClO_4)_4$, and (f) $[Cu_2(L^3)Cl_2]Cl_2$.

Table 2. Structural Parameters[a] of Copper(II) Compounds (a) $Cu(L^1)Cl]Cl$, (b) $[Cu(Me\text{-}L^1)Cl]Cl$, (c) $[Cu(Me\text{-}L^1)(NCCH_3)](BF_4)_2$, (e) $[Cu_2(L^2)(NCCH_3)_2](ClO_4)_4$, and (f) $[Cu_2(L^3)Cl_2]Cl_2$

	a	b	c	e	f
Cu−N1	2.04	2.15	2.00	2.01	2.03/2.03
Cu−N2	2.27	2.12	2.38	2.34	2.355/2.30
Cu−N3	2.02	2.06	2.075	2.01	2.01/2.03
Cu−N4	2.02	2.06	2.052	1.99	1.99/2.02
Cu−L5	2.23	2.22	1.95	1.99	2.23/2.22
N1−N2	2.92	2.93	2.93	2.93	2.91/2.92
N3−N4	3.97	4.08	4.033	3.94	3.94/3.97
Cu···Cu				7.597	7.044
N1−Cu−N2	85.02	86.71	83.68	84.56	82.84/84.41
N1−Cu−N3	81.15	82.37	81.51	82.38	81.44/81.04
N1−Cu−N4	81.25	81.63	80.90	81.82	81.20/80.22
N1−Cu−L5	165.02	112.97	174.32	175.83	169.13/168.25
N2−Cu−N3	95.35	90.26	95.66	97.38	98.40/97.59
N2−Cu−N4	95.95	91.18	99.03	92.30	90.43/93.99
N2−Cu−L5	109.95	160.31	90.93	98.50	108.03/107.34
N3−Cu−N4	158.13	163.82	155.62	160.57	159.36/156.85
N3−Cu−L5	97.36	91.68	100.87	96.37	96.53/96.79
N4−Cu−L5	96.29	92.37	98.25	98.82	98.42/98.78
C1−C2−C10−N3	86.4	77.2	95.2	86.6	93.5/90.8
C5−C4−C11−N4	90.7	−77.9	−98.7	−93	−97/−91
τ	0.115	0.059	0.312	0.25	0.16

[a] Distances in Å, angles in deg. [°].

Table 3. Cyclic Voltammetry Data for the Bispidine Copper Compounds in CH_3CN, vs $AgNO_3/Ag$[a]

complex	$E_{1/2}$ [mV]	ΔE (mV)	i_a/i_p
$[Cu(L^1)NCCH_3](BF_4)_2$	−417	134	0.85
$[Cu(Me\text{-}L^1)NCCH_3](BF_4)_2$	−98	196	0.90
$[Cu_2(L^2)(NCCH_3)_2](ClO_4)_4$	−335/−593	68/102	0.62/1.17
$[Cu_2(L^3)(NCCH_3)_2](BF_4)_4$	−400/−735	80/230	0.83/0.32

[a] 0.1 M $(Bu_4N)(PF_6)$ was used with an $Ag/AgNO_3$ reference electrode and a Pt wire as auxiliary electrode.

chromophore (mirror plane through the copper center and the two coordinated tertiary amines, i.e., one set of resonances for the pyridine donors), that of $[Cu_2(L^2)(NCCH_3)_2]^{2+}$ in acetone-d_6 shows the typical features for a coordinated ligand without mirror plane, i.e., a doubled set of signals, expected for a ligand with C_2 symmetry, as well as a characteristic downfield shift of the CH(2)/(4) signals.[54] An X-ray structural analysis of the copper(I) complex, isolated from the reaction of $[Cu(NCCH_3)_4]SbF_6$ and L^2 in acetone, shows that one of the pyridine configurations at each chromophore has been inverted (see Figure 1). It appears that in acetone a copper(I)-catalyzed retro-Mannich reaction takes place.[31,54]

Electrochemical Behavior of the Copper Compounds. Electrochemical data for $[Cu(L^1)NCCH_3]^{2+}$, $[Cu(Me\text{-}L^1)NCCH_3]^{2+}$, $[Cu_2(L^2)(NCCH_3)_2]^{4+}$, and $[Cu_2(L^3)(NCCH_3)_2]^{4+}$ are listed in Table 3. A large peak to peak separation of about 50−200 mV indicates quasi-reversible to irreversible redox processes. The solution behavior of the copper(I) bispidine complexes indicates that the misfit of bispidine ligands and copper(I) leads to labile copper(I) complexes. When the scan rate is decreased, the separations become slightly smaller, but the splitting still remains far from that expected for quasi-reversible redox processes. The redox potential of the copper complex with the α-methyl-substituted ligand $Me\text{-}L^1$ is shifted by 320 mV to a more positive potential. This confirms the previous results for the copper(II)/copper(I) redox couple of tmpa and α-alkyl-substituted tmpa complexes, respectively, where the redox couple is shifted by approximately 200−400 mV to a more positive potential.

Electronic Spectroscopy of the Copper(II) Complexes. UV−vis spectra of $[Cu_2(L^2)(X)_2]^{n+}$, $[Cu_2(Me\text{-}L^2)(X)_2]^{n+}$, $[Cu_2(L^3)(X)_2]^{n+}$, and $[Cu_2(L^4)(X)_2]^{n+}$ ($X = Cl^-$, CH_3CN) in CH_3CN have a broad, ill-resolved d−d transition at approximately 650 nm with a low-energy tail. These features are in agreement with retention of the square pyramidal geometry in solution.[55,56] The d−d absorption of $[Cu(Me\text{-}L^1)Cl]^+$ is at lower energy than for all other complexes (shift of approximately 25 nm with respect to $[Cu(Me\text{-}L^1)(NCCH_3)]^{2+}$; the intensity is roughly doubled). The low-energy shift indicates retention of the observed solid state coordination geometry in solution, i.e., coordination of Cl^- trans to N7, with a square pyramidal structure and a quenched Jahn−Teller distortion. This also emerges from DFT-calculations.[35] In contrast, with the sterically less demanding $NCCH_3$ donor, the electronically preferred coordination in-plane with the pyridine donors and N3 is possible, and the UV−vis spectra of $[Cu(L^1)(NCCH_3)]^{2+}$ and $[Cu(Me\text{-}L^1)(NCCH_3)]^{2+}$ are essentially identical. In accordance with results from DFT calculations, this indicates that the preferred copper(II) coordination geometry, leading to stable complexes with strong Cu−substrate bonds (Cl^-, $NCCH_3$, peroxide), has copper(II) in-plane with N3, the two pyridine donors, and the substrate, with a long bond to N7, and the two pyridine groups roughly coplanar to the Cu−N3−substrate plane.[35]

Solution Conductivity of the Copper(II) Compounds. The molar conductivities of copper(II) compounds of the ligands L^1−L^4 were measured in acetonitrile at rt. The molar conductivities Λ_M of the chloro complexes with ligand L^1 and $Me\text{-}L^1$ are typical for 1:1 electrolytes[57] (196.0 $cm^2\ \Omega^{-1}\ mol^{-1}$ for $[Cu(L^1)Cl]Cl$, 115.3 $cm^2\ \Omega^{-1}\ mol^{-1}$ for $[Cu(Me\text{-}L^1)Cl]Cl$), indicating that chloride remains coordinated to copper(II) in solution. For $[Cu(L^1)(NCCH_3)](ClO_4)_2$ and $[Cu(Me\text{-}L^1)(NCCH_3)](ClO_4)_2$, the higher conductivity Λ_M shows that the complexes are dissolved as dications (335.1 and 355.5 $cm^2\ \Omega^{-1}\ mol^{-1}$, respectively). Therefore, the solid state structures of these compounds are also retained in acetonitrile. The behavior of the dinuclear complexes with the ligands L^2, L^3, and L^4 is similar, and this indicates that in solution these dinuclear complexes exist either as dications ($[Cu_2(L^n)Cl_2]^{2+}$, $n = 2, 3, 4$; 239.1 $cm^2\ \Omega^{-1}\ mol^{-1}$ for $[Cu_2(L^2)Cl_2]^{2+}$, 140.7 $cm^2\ \Omega^{-1}\ mol^{-1}$ for $[Cu_2(L^3)Cl_2]^{2+}$, 174.0 $cm^2\ \Omega^{-1}\ mol^{-1}$ for $[Cu_2(L^4)Cl_2]^{2+}$) or as tetracations ($[Cu_2(L^n)(NCCH_3)_2]^{4+}$, $n = 2, 3, 4$; 453.7 $cm^2\ \Omega^{-1}\ mol^{-1}$ for $[Cu_2(L^2)(NCCH_3)_2]^{4+}$, 406.1 $cm^2\ \Omega^{-1}\ mol^{-1}$ for $[Cu_2(L^3)(NCCH_3)_2]^{4+}$, 435.5 $cm^2\ \Omega^{-1}\ mol^{-1}$ for $[Cu_2(L^4)(NCCH_3)_2]^{4+}$). The low conductivities of $[Cu_2(L^3)Cl_2]^{2+}$ and $[Cu_2(L^4)Cl_2]^{2+}$

(54) Boerzel, H.; Comba, P. Unpublished.

(55) Lever, A. B. P. *Inorganic Electron Spectroscopy*, 2nd ed.; Elsevier: New York, 1986.
(56) Wei, N.; Murthy, N. N.; Karlin, K. D. *Inorg. Chem.* **1994**, *33*, 6093.
(57) Huheey, J. E. *Inorganic chemistry—Principles of structure and reactivity*, 2nd ed.; Harper & Row: New York, 1978.

are possibly due to a weak interaction between a third chloride and the dichlorodicopper(II) complexes.

Oxygenation of the Copper(I) Complexes. In solution the copper(I) complexes of L^n, $n = 1, 2, 3, 4$, are very air-sensitive and react with molecular oxygen with immediate formation of deep-purple peroxo dicopper(II) compounds.[32] In contrast, when the copper(I) complexes $[Cu(Me\text{-}L^1)]^+$ and $[Cu_2(Me\text{-}L^2)]^{2+}$ are left in air, a color change from yellow to green-blue occurs over several hours. We could not detect any peroxo dicopper(II) compounds in these oxidation reactions with the copper(I) complexes of the methylated bispidine ligands. It emerges that in-plane coordination of dioxygen is prevented by the methyl substituents, and axial interaction with dioxygen does not lead to stable peroxo compounds (see also above and ref 35). This is also supported by the more positive redox potentials of the copper complexes with Me-L^1 compared to the copper complexes with L^1, i.e., the copper(II) form is destabilized with the methylated ligands. Note that changes in oxygenation reactivity have also been observed with tmpa, α-methyl-substituted tmpa, and corresponding quinolyl-substituted ligands.[30,58] Note that, while in both cases steric influences are the basis for the differences in reactivity, in the bispidine systems discussed here, this leads to two different chromophores with considerable differences in electronic properties.

The thermal stability of the peroxo dicopper(II) compounds with L^1−L^4 depends on the nature of the spacer group between the two bispidine cavities; while $[Cu(L^1)NCCH_3]^+$ (mononucleating ligand) reacts with dioxygen to form superoxo and peroxo species, observable at low temperatures in stopped-flow experiments (vide infra), the peroxo dicopper(II) compounds of L^2−L^4 differ drastically in terms of their thermal stabilities. The stability of the peroxo complex generated by oxygenation of $[Cu_2(L^3)(NCCH_3)_2]^{2+}$ is comparable to that obtained by oxygenation of the corresponding copper(I) complex with L^1 ($t_{1/2}$ (250 K) = 15 s); the compounds obtained by oxygenation of the copper(I) compounds with the more rigid ligands L^2 and L^4 are fairly stable under ambient conditions ($t_{1/2}$ (298 K) = 10 and 50 min, respectively; spectrophotometric analyses, decrease of the LMCT transitions). The UV−vis spectra of the oxygenation products of the copper(I) bispidine compounds are typical for *trans*-μ-1,2-peroxo−dicopper(II) complexes, with a dominant LMCT band at approximately 510 nm and a low-energy shoulder at approximately 600−650 nm (see Table 4). The transition energies differ only marginally for the series of bispidine compounds, and the major transitions occur at significantly higher energy than the LMCT transitions for other *trans*-μ-1,2-peroxo−dicopper(II) complexes (see Table 4). The extinction coefficients (derived from stopped-flow data, vide infra) are smaller than those of other systems.

Dioxygen binds irreversibly to the copper(I) bispidine compounds, oxidizing the metal center to copper(II). There are examples where a decreasing of the pressure, slight warming of the solution, or addition of PPh_3 releases dioxygen from peroxo−dicopper(II) compounds,[10,13,17,30] but this is not possible with the present compounds. Irreversible dioxygen binding may be due to very strong Cu^{II}−O_2^{2-} bonding. The energy of the LMCT transition is a good criterion for the ease of electron transfer from peroxide to copper(II); with low-energy LMCT transitions electron transfer from peroxide to copper(II) is facile and indicates that reversible dioxygen binding is, in principle, possible. Thus,the high-energy transitions of the bispidine compounds are in agreement with the irreversibility of the peroxo compound formation. However, irreversible oxygen binding can also have other reasons, such as the formation of polymeric $Cu-O_2$ species.[12]

Table 4. Charge Transfer (nm) and Raman (ν_{O-O}, cm^{-1}) Transitions of Peroxo Dicopper(II) Compounds

	CT	CTsh	ν_{O-O}
$[Cu_2(L^1)_2O_2]^{2+}$	504	630	840
$[Cu_2(L^2)O_2]^{2+}$	488	649	824
$[Cu_2(L^3)O_2]^{2+}$	499	650	837
$[Cu_2(L^4)O_2]^{2+}$	503	650	847
$[Cu_2(tmpa)_2O_2]^{2+}$ [a,b]	525	590	832

[a] References 10, 69, and 70. [b] Ethyl-bridged bis-tmpa.

Raman Spectroscopy of the μ-Peroxo Dicopper(II) Compounds. FT and resonance Raman experiments were performed in CH_3CN solutions of the copper(I) complexes, after bubbling dioxygen for about 30 s at −40 °C through the solutions.[32,59] For the peroxo complexes of L^2 and L^4, the O−O stretching frequencies occur at 824 cm^{-1} (L^2) and 847 cm^{-1} (L^4); for the complex with L^1, the stretching frequency is at 840 cm^{-1}, and for that with L^3, at 837 cm^{-1}. The bands are broad, and it cannot be excluded that they consist of several unresolved transitions. Note that the low energy of the O−O stretching transition is correlated with the energy of the LMCT band and with the rate of decay (stability) of the peroxo compounds (with the exception of the peroxo product of L^4). In complexes were reversible dioxygen binding has been observed (e.g., with tmpa and bridged bis-tmpa ligands) the energy of the O−O stretching transition occurs at around 832 cm^{-1}.[60] As pointed out above, the LMCT band of the peroxo compounds obtained by oxygenation of copper(I) bispidine complexes indicates the ease of electron transfer from O_2^{2-} to copper(II) and decreases in the order $L^2 > L^3 > L^1 \sim L^4$, and the strength of the O−O bond decreases in the inverse order, i.e., $L^4 > L^1 > L^3 > L^2$.

Reactivity of the μ-Peroxo Dicopper(II) Compounds. The copper peroxo compounds do not lead to hydroxylation or oxidation of the ligand backbone: when an oxygenated solution of $[Cu_2(L^4)(NCCH_3)_2]^{2+}$ was treated with NH_4OH/CH_2Cl_2 to extract the ligand from the solution, only the original ligand L^4 could be isolated (^1H NMR, FAB^+-MS; recovery of 30%, due to the solubility of the ligand). Characteristic for *trans*-μ-1,2-peroxo-compounds is their

(58) Hayashi, H.; Fujinami, S.; Nagatomo, S.; Ogo, S.; Suzuki, M.; Uchara, A.; Watanabe, Y.; Kitagawa, T. *J. Am. Chem. Soc.* **2000**, *122*, 2124.
(59) Börzel, H. Ph.D. Thesis, University of Heidelberg, **2000**.
(60) Baldwin, M. J.; Ross, P. K.; Pate, J. E.; Tyeklar, Z.; Karlin, K. D.; Solomon, E. I. *J. Am. Chem. Soc.* **1991**, *113*, 8671.

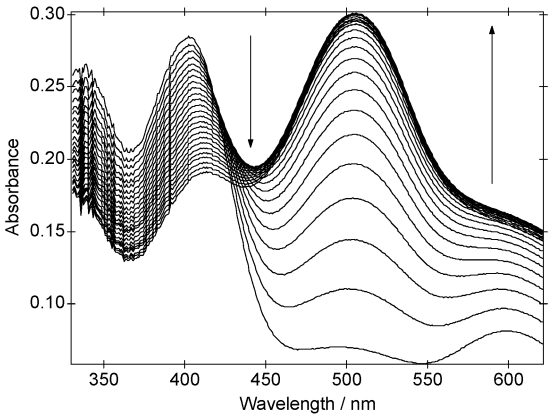

Figure 3. Reaction of $[Cu(L^1)(NCCH_3)]^+$ with dioxygen at −90 °C in propionitrile ([complex] = 0.2 mM, $[O_2]$ = 4.4 mM, Δt = 0.27 s, total time is 7 s).

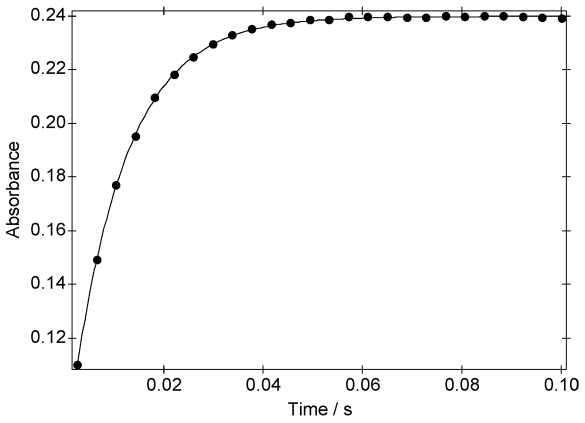

Figure 4. Absorbance vs time trace at 404 nm (solid line: fit to one exponential function) for the reaction of $[Cu(L^1)(NCCH_3)]^+$ with dioxygen at −90 °C in propionitrile ([complex] = 0.2 mM, $[O_2]$ = 4.4 mM).

basic nature: quantitative deprotonation of catechol occurs in solutions of these complexes.[36] Their stability is drastically reduced in the presence of protic solvents, where they decompose about 10 times faster than in an aprotic environment. Upon a dropwise addition of H_2O to a solution (propionitrile) of the copper(II) peroxo complex of L^2, the solution rapidly turns brown, with the absorption spectrum showing features at 358, 478, and 620 nm. The 358 nm band is assigned to a HO→copper(II) charge transfer transition,[61] with OH^- being formed by protonation and cleavage of the peroxo bond.

Time-Resolved UV−Vis Spectra during the Oxygenation Process. Stopped-flow experiments were carried out in propionitrile and acetone to investigate the dioxygen intermediates during the formation of the peroxo complexes, e.g., the copper(II) superoxo compounds which were unobservable in the benchtop experiments (eq 1). Such short-lived intermediates were observed at low temperatures and/or upon exchange of the nitrile solvent for acetone, a procedure used in previous studies to stabilize copper(II) peroxo compounds.[40,44]

$$[LCu^{I}{-}NCCH_3]^+ + O_2 \leftrightarrows [LCu^{II}{-}O_2^-]^+ + CH_3CN$$

$$[LCu^{II}{-}O_2^-]^+ + [LCu^{I}{-}NCCH_3]^+ \leftrightarrows [LCu^{II}{-}O_2^{2-}{-}Cu^{II}L]^{2+} \quad (1)$$

Time-resolved UV−vis spectra of the reaction of $[Cu(L^1)(NCCH_3)]BF_4$ with O_2 (pseudo-first-order conditions, $[O_2] \gg$ [complex]) at −90 °C in propionitrile are shown in Figure 3. These spectra provide evidence for the formation of $[Cu(L^1)O_2]^+$ and $[(L^1)CuO_2Cu(L^1)]^{2+}$. The spectral features are very similar to those of the known UV−vis spectra of superoxocopper(II) and peroxo-dicopper(II) complexes.[44,62] The absorbance maxima of the superoxo compound $[Cu(L^1)O_2]^+$ (LMCT at 404 nm (8000 M^{-1} cm^{-1}), shoulder at 599 nm (3000 M^{-1} cm^{-1})) and of the peroxo complex $[(L^1)Cu(O_2)Cu(L^1)]^{2+}$ (LMCT 504 nm (8000 M^{-1} cm^{-1}) and shoulder at >620 nm (5400 M^{-1} cm^{-1})) were assigned accordingly and as discussed above; resonance Raman studies also support the assignment of the product as $[(L^1)Cu(O_2)Cu(L^1)]^{2+}$.[31]

The formation of the superoxo complex $[Cu(L^1)O_2]^+$ can be observed prior to the formation of the peroxo product when rapid measuring times are used. Figure 4 shows an absorbance vs time trace at 404 nm. This trace could be fitted to a single-exponential function with an observed rate constant k_{obs} of 90 ± 15 s^{-1}. Assuming an overall second-order rate law, d[superoxo complex]/dt = k[copper(I) complex][O_2], a second-order rate constant of approximately 20000 M^{-1} s^{-1} at −90 °C is obtained. This is similar to that obtained in a detailed kinetic study of the reaction of $[Cu(tmpa)(NCCH_3)]^+$ with dioxygen.[62] Longer reaction times show that the superoxo complex decays fast (−90 °C: approximately 70 s) At higher temperatures (−70 °C), only the formation and subsequent decay of the peroxo-dicopper(II) complex was observed.

In contrast to the mononuclear superoxo compound generated by oxygenation of $[Cu(L^1)(NCCH_3)]^+$, oxygenation of $[Cu_2(L^3)(NCCH_3)_2]^{2+}$ allowed only the formation of the peroxo dicopper(II) compound to be observed. This can be explained by a rate-determining formation of the superoxodicopper(II) complex, followed by a fast consecutive reaction to the peroxo product. This has absorption maxima at 499 nm (6800 M^{-1} cm^{-1}) with a shoulder at >620 nm, and a high-energy shoulder at 425 nm (2600 M^{-1} cm^{-1}). Even at −90 °C the peroxo complex starts to decompose after 0.5 s.

The oxygenation behavior of $[Cu_2(L^4)(NCCH_2)_2]^{2+}$ is different again. At low temperature (−90 °C), the formation of two LMCT bands can be observed at 425 and 503 nm, with a shoulder at >620 nm and an additional transition at 345 nm. The transitions at 345 and 425 nm are not observable at T > −50 °C and are therefore attributed to labile intermediates. The band at 425 nm in the low-temperature spectrum might be due to a superoxo species; however, this would be unusual, because the intensity of the band at 425 nm grows simultaneously with that attributed to the peroxo complex (503 nm). In previous studies, only formation of

(61) Casella, L.; Carugo, O.; Gullotti, M.; Garofani, S.; Zanello, P. *Inorg. Chem.* **1993**, *32*, 2056.
(62) Karlin, K. D.; Wei, N.; Jung, B.; Kaderli, S.; Niklaus, P.; Zuberbühler, A. D. *J. Am. Chem. Soc.* **1993**, *115*, 9506.

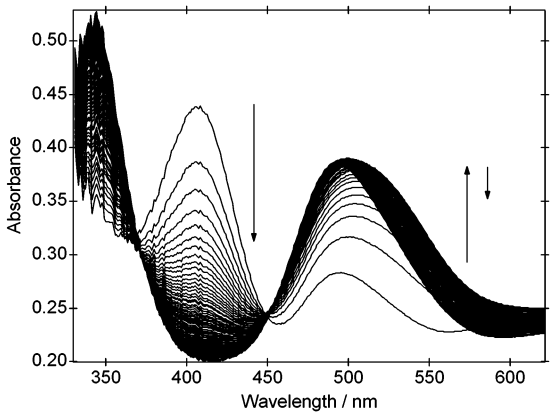

Figure 5. Reaction of $[Cu_2(L^2)(NCCH_3)_2]^{2+}$ with dioxygen at −60 °C in acetone ([complex] = 0.2 mM, $[O_2]$ = 5.1 mM, Δt = 1.2 s, total time is 100 s).

the superoxo complex, followed by its decomposition and subsequent formation of the peroxo complex, has been observed. There are at least two possible explanations: (i) At low temperature the rate of the formation and decay of the superoxo compound are similar, and with increasing temperature decomposition is faster. (ii) There is formation of intermolecular dioxygen adducts. At higher temperature only formation of peroxo dicopper(II) products is observed (503 nm (6000 M^{-1} cm^{-1}), 423 nm (sh), 620 nm (sh, −2400 M^{-1} cm^{-1})). The rate of formation increases with higher temperature; equilibrium is reached at −70 °C in approximately 30 ms, at −50 and −20 °C in approximately 10 ms, indicating a positive enthalpy of formation.

The most interesting system is that of $[Cu_2(L^2)NCCH_3)_2]^{2+}$, and this leads to the most stable peroxo dicopper(II) compound with bispidine ligands when reacted with dioxygen, and to one of the most stable μ-peroxo-dicopper(II) compounds known so far. The oxidation reaction of the copper(I) precursor, dissolved in acetone, allowed detection of a copper(II) superoxo complex with CT bands at 405 nm (530 M^{-1} cm^{-1}), 487 nm (270 M^{-1} cm^{-1}), and 605 nm (240 M^{-1} cm^{-1}). This decays slowly (−90 °C), and a peroxo complex is formed (488 nm (230 M^{-1} cm^{-1}), >620 nm (sh, 170 M^{-1} cm^{-1})). As shown in Figure 5, the decay is faster at higher temperatures, and, furthermore, the initial peroxo complex is converted to another peroxo species, with spectroscopic features similar to those of the species observed, when the reaction is carried out in propionitrile (see below; hypsochromic shift 495 → 487 nm).

When a solution of the copper(I) complex is oxygenated at low temperature in propionitrile, no transient superoxo species can be observed. Instead, only a species with absorption maxima at 482 nm (3040 M^{-1} cm^{-1}) and >620 nm (sh, 1800 M^{-1} cm^{-1}) is observed (for comparison: oxygenation at rt leads to a species with spectroscopic features at 492 nm (3000 M^{-1} cm^{-1}), with a shoulder at >620 nm (1800 M^{-1} cm^{-1})). However, when this reaction is followed at low temperature over a longer period of time (8.5 min), an unexpected change in the UV−vis spectrum occurs: the first spectrum, recorded immediately after mixing, shows the above-mentioned features; the second spectrum, obtained after 12 s, shows different features, and the following spectra stay approximately constant for the next 8.5 min (maximum time span). The intensity of the 485 nm transition and the shoulder at 620 nm decrease with an absorption band at 354 nm growing in intensity (3400 M^{-1} cm^{-1}). The absorption maximum is shifted from 482 to 467 nm, and over the following 8.5 min back to 474 nm (2200 M^{-1} cm^{-1}). The intensity of the band at 354 nm remains approximately constant. When the temperature is increased stepwise from −70 to 0 °C, a similar behavior is observed, i.e., formation of a band around 475 nm (±5 nm), shifting to lower energy with time (485 nm (± 5 nm)). At 273 K, the spectrum is very similar to the rt spectrum. The rate of formation decreases with increasing *T*, indicating a negative enthalpy of formation (note the different behavior to $[Cu_2(L^4)O_2]^{2+}$).

Conclusion

The work presented here demonstrates that bispidine-type ligands are well suited for the stabilization of copper superoxo and dicopper peroxo compounds. Mononuclear $[Cu(L^1)(NCCH_3)]^+$ was found to react with O_2, in a similar way to $[Cu(tmpa)(NCCH_3)]^+$, forming a dinuclear *trans*-μ-peroxo complex. However, in contrast to the trigonal bipyramidal geometry of $[(tmpa)CuO_2Cu(tmpa)]^{2+}$ with the peroxo ligand in the axial position, the geometry of $[(L^1)CuO_2Cu(L^1)]^{2+}$ is distorted square pyramidal with the peroxo ligand occupying an equatorial position. No crystal structure of the peroxo complex is available to date, but the structure can be inferred from other structurally characterized copper(II) complexes of this ligand, e.g., $[Cu(L^1)(Cl)]Cl$,[32] as has been found for copper tmpa complexes.[63] Also, this structural assignment is supported by model calculations, using both force field and DFT models.[32,35] This notable structural difference is important because a peroxo ligand in the axial position of a square pyramidal copper complex would be very labile toward substitution. This is one of the reasons why it was impossible to observe oxygenation products during the oxidation of $[Cu(Me\text{-}L^1)(NCCH_3)]^+$ and $[Cu(Me\text{-}L^2)(NCCH_3)_2]^{2+}$. Similar observations were made with [Cu(trien)], where the peroxo ligand would also be axially coordinated in a square pyramidal product complex.[64]

Even at low temperatures $[(L^1)CuO_2Cu(L^1)]^{2+}$ is not very persistent, but the stability of the copper peroxo species can be enhanced dramatically by connecting two mononuclear units with various bridges. The most interesting system in the investigated series is derived from $[Cu_2(L^2)(NCCH_3)_2]^{2+}$, which leads to the most stable peroxo dicopper(II) compound when reacted with dioxygen; however, the spectroscopic studies indicate that the high stability could also be due to intermolecular reactions, as observerd for other dinuclear complexes.[10,11,65]

(63) Karlin, K. D.; Hayes, J. C.; Juen, S.; Hutchinson, J. P.; Zubieta, J. *Inorg. Chem.* **1982**, *21*, 4106.
(64) Becker, M.; Heinemann, F.; Knoch, F.; Donaubauer, W.; Liehr, G.; Schindler, S.; Golub, G.; Cohen, H.; Meyerstein, D. *Eur. J. Inorg. Chem.* **2000**, 719.
(65) Pidcock, E.; Obias, H. V.; Masaaki, A.; Liang, H.-C.; Karlin, K. D.; Solomon, E. I. *J. Am. Chem. Soc.* **1999**, *121*, 1299.

Experimental Section

Materials and Methods. Reagents and solvents were of commercially available reagent quality. Air-sensitive compounds were prepared and handled in a glovebox (N_2 or Ar) or with standard Schlenck techniques. Solvents were deoxygenated by bubbling inert gases through the solution or by two freeze−pump−thaw cycles. Elemental analyses were obtained from the microanalytical laboratory of the Chemical Institutes at the University of Heidelberg or by Atlantic Microlabs, Inc., Atlanta, GA. Infrared spectra were recorded as KBr disks on a Perkin-Elmer 16C instrument. NMR spectra were measured on a Bruker AC200, a General Electric QE300, a Bruker WH300, a Bruker Spectrospin DRX 500, or an Omega 600 instrument. Chemical shifts are reported as δ values downfield from an internal standard of TMS. UV−vis spectra were measured on a Varian Cary 1E UV−vis spectrometer in quartz cuvettes with 1 cm path length. Electric conductivity measurements were carried out in CH_3CN with a Knick conductivity bridge. Cyclic voltammetry (CV) measurements were recorded on a BAS 100B instrument with a standard three-electrode cell (glassy carbon working electrode, $Ag/AgNO_3$ reference electrode (0.01 M $AgNO_3$), Pt wire auxiliary electrode) at room temperature in degassed CH_3CN in an Ar atmosphere; tetrabutylammonium hexafluorophosphate (0.1 M) was used as supporting electrolyte in 50-fold excess, with respect to the corresponding copper(II) complexes (2 mmol). Scan rates were between 20 mV s^{-1} and 1 V s^{-1}. The potential of the Fc^+/Fc couple at a scan rate of 100 mV s^{-1} lies at 87 mV with $\Delta E = 64$ mV.

Variable-Temperature Stopped-Flow Measurements. Solutions of complexes for the collection of time-resolved UV−vis spectra were prepared in a glovebox and transferred with syringes to the low-temperature stopped-flow instrument. A dioxygen-saturated solution was prepared by bubbling dioxygen through propionitrile or acetone in a syringe (solubility of dioxygen at 25 °C: propionitrile, 0.0088 M;[62] acetone, 0.0102 M[66]). Time-resolved UV−vis spectra of the reactions of dioxygen with the copper(I) complexes were recorded with a modified Hi-Tech SF-3L low-temperature stopped-flow unit (Salisbury, U.K.), equipped with a J&M TIDAS 16-500 photodiode array spectrophotometer (J&M, Aalen, Germany). Data treatment was carried out with the integrated J&M software Kinspec or the program Specfit (Spectrum Software Associates, Chapel Hill, NC).

Ligand Syntheses. The ligands L^1, Me-L^1, and L^2, as well as the piperidone precursor pL^1 and Me-pL^1 (for ligand structures see Chart 1), were prepared according to methods described previously.[32,67]

Me-L^2: similar to L^2, from the piperidone precursor Me-pL^1 (2.43 mmol, 1 g), 37% aqueous HCHO solution (5.8 mmol, 0.53 mL), and 1,2-diaminoethane (1.46 mmol, 0.12 mL) in THF (8 mL). After removal of $^2/_3$ of the solvent in vacuo, and storage of the remaining reaction mixture for 2 days at 5 °C, the product could be isolated as a yellowish powder. Yield: 90 mg (6.6%); $C_{50}H_{58}N_8O_{10}$ (931.06). FAB^+-MS (Nibeol): 931 (M^+; 40%); 465 ($M/2^{2+}$; 100%). ^1H NMR (300 MHz, $CDCl_3$): 7.89 (d; $^3J = 7.8$ Hz), 7.34 (t; $^3J = 7.8$ Hz), 7.15 (d; $^3J = 7.2$ Hz), 4.7 (H2/H4), 3.9 (H6/8(eq)), 3.68 (OCH_3), 2.9 (H6/8(ax)), 2 (N7−CH_3), 1.99 (N3−CH_3). ^{13}C NMR (75 MHz, $CDCl_3$): 62.16 (C1, C5), 73.33 (C2,C4), 59.47 (C6/C8), 43.57 (N3−CH_3), 52.30 (O−CH_3), 168.81 (C═O).

L^3: according to the synthesis of L^2 from piperidone pL^1 (15.7 mmol, 6 g), 37% aqueous HCHO solution (37.6 mmol, 3.38 mL), and 1,3-diaminopropane (9.4 mmol, 0.82 mmol) in THF (40 mL). Yield: 5.23 g (5.89 mmol, 75%). $C_{47}H_{52}N_8O_{10}$ (888.98), calcd (found): C 63.50 (63.00), H 5.90 (6.02), N 12.60 (12.45). FAB^+-MS (Nibeol): 889 (M + 1; 100%). ^1H NMR (300 MHz, $CDCl_3$): 7.13 (td; $^3J = 5.16$ Hz, PyH3), 7.65 (td; $^3J = 6.8$ Hz; $^4J = 1.4$ Hz, PyH4), 7.93 (d; $^3J = 8$ Hz, PyH5), 8.47 (d; $^3J = 3.6$ Hz, PyH6), 2.00 (N3−CH3), 3.83 (OCH3), 4.69 (H2/H4), 3.08 ($^2J = 12$ Hz, H6/H8(eq)), 2.63 ($^2J = 12$ Hz, H6/H8(ax)), 2.36 (t, N−CH_2, $^3J = 7.6$ Hz), 1.5 (m, N−CH_2−CH_2−). ^{13}C NMR (75 MHz, $CDCl_3$): 62.04 (C1/C5), 73.47 (C2/C4), 58.48 (C6/C8), 42.89 (N3−CH_3), 52.30 (OCH_3), 203.21 (C(9), 168.52/158.26 (C═O).

L^4: The piperidone pL^1 (34 mmol, 13 g) is dissolved upon slight warming in MeOH (120 mL). To this solution is added slowly 37% HCHO solution (81.6 mmol, 7.3 mL) and *m*-xylylene diamine (20.4 mmol, 2.64 mL). The solution turns dark brown upon addition of the amine. The reaction mixture is refluxed at 85 °C for 1 h. After removal of the solvent in vacuo, 12 mL of EtOH is added to the black tarlike residue, which dissolves to form a dark brown solution. After 2 h, the product precipitates from the solution as a greenish powder, which can be filtered off and washed portionwise with small amounts of cold EtOH. Drying in vacuo leads to 4.38 g (4.6 mmol, 27%) of analytically pure off-white product. $C_{52}H_{54}N_8O_{10}$ (951.05), calcd (found): C 65.68 (65.22), H 5.68 (5.71), N 11.79 (11.80). ^1H NMR (300 MHz, CD_3CN): 2.23 (N3−CH_3), 3.72 (OCH_3), 4.60 (H2/H4), 3.06 ($^2J = 12.4$ Hz, H6/H8(eq)), 2.54 ($^2J = 12$ Hz, H6/H8(ax)), 2.16 (s, CH_2-*m*-xylyl), 7.16 (m, PyH3), 7.57 (td; $^3J = 7.7$ Hz; $^4J = 1.8$ Hz, PyH4), 7.88 (d; $^3J = 7.9$ Hz, PyH5), 8.40 (d; $^3J = 4$ Hz, PyH6). ^{13}C NMR (75 MHz, CD_3CN): 61.82 (C1/C5), 73.40 (C2/C4), 58.26 (C6/C8), 42.82 (N3−CH_3), 52.30 (OCH_3), 203.10(C(9), 168.33 (C═O).

Synthesis of Copper(I) Complexes. [Cu(L^1)NCCH$_3$]X (X = BF_4^-, $CF_3SO_3^-$). A solution of $[Cu(CH_3CN)_4]X$ (X = BF_4^-, $CF_3SO_3^-$) (0.23 mmol) in 1 mL of CH_3CN is added to a suspension of L^1 (100 mg, 0.23 mmol) in CH_3CN (1 mL). Acetonitrile may be substituted by acetone if X = BF_4^-. The complexes can be isolated as red (X = BF_4^-) or yellow crystals (X = $CF_3SO_3^-$) by diethyl ether diffusion into the solution.

[Cu(L^1)NCCH$_3$]BF_4. $C_{25}H_{29}N_5O_5CuBF_4$ (629.66), calcd (found in the product isolated (i) from CH_3CN, (ii) from acetone): C 47.67 ((i) 47.30, (ii) 47.46), H 4.64 ((i) 4.70, (ii) 4.75), N 11.12 ((i) 11.17, (ii) 11.02). IR (KBr) [cm^{-1}]: 2954, 2869, 2811 (m), 1737 (vs), 1598 (s), 1573 (m), 1439 (s), 1275 (vs), 962 (m), 776 (m), 560 (m).

[Cu(L^1)NCCH$_3$]CF_3SO_3. $C_{26}H_{29}N_5SO_8CuF_3$ (691.92), calcd (found): C 45.12 (44.90), H 4.22 (4.07), N 10.12 (9.87). IR (KBr) [cm^{-1}]: 2952 (m), 2669 (m), 2812 (m), 1739 (vs), 1599 (s), 1588 (s), 1571 (m), 1441 (vs), 1261 (vs), 1023 (vs), 780 (vs), 966 (m).

[Cu(Me-L^1)]OTf. $C_{26}H_{30}N_5O_8CuF_3S$ (679.15), calcd (found): C 45.98 (45.85), H 4.45 (4.43), N 8.25 (8.36).

[Cu$_2$(L^2)(NCCH$_3$)$_2$]X$_2$ (X = BF_4^-, OTf^-, SbF_6^-). A solution of $[Cu(CH_3CN)_4]X$ (X = BF_4^-, OTf^-, SbF_6^-) (0.23 mmol) in 1 mL of CH_3CN is added to a suspension of L^2 (100 mg, 0.115 mmol) in CH_3CN (1 mL). Acetonitrile was substituted by the double volume of acetone for X = SbF_6^-. The complexes can be isolated as yellow-brownish powders or as a light yellow crystalline material (X = SbF_6^-) upon diethyl ether diffusion at rt into the solution.

[Cu$_2$(L^2)(NCCH$_3$)$_2$](BF$_4$)$_2$. $Cu_2C_{50}H_{56}O_{10}N_{10}B_2F_8$ (1257.75), calcd (found): C 47.75 (47.48), H 4.49 (4.49), N 11.14 (11.02).

[Cu$_2$(L^2)(NCCH$_3$)$_2$](OTf)$_2$. $Cu_2C_{52}H_{56}O_{16}N_{10}S_2F_6$ (1382.28), calcd (found): C 45.18 (45.10), H 4.08 (4.22), N 10.13 (10.01).

The copper(I) complexes of Me-L^2 were prepared in situ by mixing 1 equiv of Me-L^2 and 2 equiv of $[Cu(CH_3CN)_4]X$ (X = BF_4^-, ClO_4^-) in CH_3CN.

(66) Lühring, P.; Schumpe, A. *J. Chem. Eng. Data* **1989**, *34*, 250.
(67) Holzgrabe, U.; Erciyas, E. *Arch. Pharm.* **1992**, *325*, 657.

Table 5. X-Ray Crystal Structure Data

	$[Cu_2(L^3)(NCCH_3)_2](PF_6)_2$	$[Cu_2(L^2)(NCCH_3)_2](SbF_6)_2$	$[Cu_2(L^2)(NCCH_3)_2](ClO_4)_4$	$[Cu_2(L^3)Cl_2]Cl_2$
empirical formula	$C_{53}H_{61}ClCu_2F_6N_{11}O_{14}P$	$C_{50}H_{56}Cu_2F_{12}N_{10}O_8Sb_2\cdot 0.8$acetone	$C_{58}H_{72}Cl_4Cu_2N_{14}O_{28}$	$C_{51}H_{66}Cl_4Cu_2N_{10}O_{14}$
fw	1383.63	1597.26	1682.18	1312.02
cryst syst	triclinic	triclinic	monoclinic	monoclinic
space group	$P\bar{1}$	$P\bar{1}$	$P2_1/n$	$C2/c$
unit cell dimensions [Å] [deg]	$a = 12.4528(2)$	$a = 11.2146(7)$	$a = 12.2689(5)$	$a = 39.66(2)$
	$b = 13.5325(2)$	$b = 13.1737(8)$	$b = 22.5707(9)$	$b = 17.754(9)$
	$c = 20.6999(4)$	$c = 13.8585(9)$	$c = 13.8972(6)$	$c = 17.745(9)$
	$\alpha = 71.013(1)$	$\alpha = 64.625(1)$	$\alpha = 90$	$\alpha = 90$
	$\beta = 74.294(1)$	$\beta = 68.624(1)$	$\beta = 113.438(1)$	$\beta = 109.89(2)$
	$\gamma = 65.584(1)$	$\gamma = 68.390(1)$	$\gamma = 90$	$\gamma = 90$
V [Å^3]	2965.71(1)	1667.01(18)	3530.9(3)	11749(10)
Z	2	1	2	8
density (calcd) [g cm^{-3}]	1.549	1.59	1.582	1.483
absn coeff [mm^{-1}]	0.882	1.524	0.848	0.977
F(000)	1424	795	1736	5440
cryst size [mm^3]	0.32 × 0.25 × 0.16	0.3 × 0.2 × 0.2	0.30 × 0.30 × 0.27	0.40 × 0.16 × 0.09
indept reflns	12131	7921	7219	7193
params	778	453	527	737
GOF on F^2	1.076	1.045	1.050	1.009
final R indices [$I > 2\sigma(I)$]	R1 = 0.0857	R1 = 0.0577	R1 = 0.0427	R1 = 0.0590
R indices (all data)	wR2 = 0.2749	wR2 = 0.1956	wR2 = 0.1193	wR2 = 0.1546
largest diff peak/hole [e Å^{-3}]	1.917/−2.144	1.147 and −1.024	1.180/−0.486	0.706/−0.470

$[Cu_2(L^3)(NCCH_3)_2]X_2$ ($X^- = BF_4^-$, OTF^-). Dicopper(I) complexes were prepared similarly to the dicopper(I) complexes of L^2. The origin of the water is unclear.

$[Cu_2(L^3)(NCCH_3)_2](BF_4)_2\cdot 2H_2O$. $Cu_2C_{52}H_{64}O_{12}N_{10}B_2F_8$ (1321.75), calcd (found): C 46.46 (46.42), H 4.69 (4.65), N 9.95 (10.28).

$[Cu_2(L^3)(NCCH_3)_2](CF_3SO_3)_2\cdot 2H_2O$. $Cu_2C_{54}H_{64}O_{18}N_{10}S_2F_6$ (1446.28), calcd (found): C 44.03 (44.16), H 4.27 (4.13), N 9.06 (9.45).

$[Cu_2(L^4)(NCCH_3)_2](BF_4)_2\cdot 2H_2O$. The copper(I) complex was prepared in an analogous fashion to the dicopper(I) complexes of L^2. $Cu_2C_{52}H_{58}N_8O_{12}B_2F_8$ (1287.78), calcd (found): C 48.50 (48.17), H 4.54 (4.47), N 8.70 (8.96).

Synthesis of Copper(II) Complexes. $[Cu(L^1)Cl]Cl\cdot H_2O$. $CuCl_2\cdot 2H_2O$ (78.4 mg) in 2 mL of dry CH_3CN was added to a suspension of L^1 (200 mg, 0.46 mmol) in 2 mL of dry CH_3CN. The resulting blue solution was put in a diethyl ether diffusion bath. After 1 day, blue crystals precipitated from the solution. $CuC_{23}H_{28}N_4O_6Cl_2$ (590.95), calcd (found): C 46.75 (46.32), H 4.78 (5.05), N 9.48 (9.77). FAB^+-MS (Nibeol): 554 ($[Cu(L^1)Cl\cdot H_2O]^+$, 100%); 536 ($[Cu(L^1)Cl]^+$; 18%); 519 ($[Cu(L^1)H_2O]^+$; 10%). IR [cm^{-1}]: 2922, 2852 (s), 1733 (vs), 1616, 1606 (m), 1464 (m), 1267, 1245 (m), 1066, 1046, 1026 (m), 783 (m).

$[Cu(L^1)](ClO_4)_2\cdot 2H_2O$. $[Cu(H_2O)_6](ClO_4)_2$ (85 mg) in 1 mL of CH_3CN is added to a suspension of L^1 (100 mg, 0.23 mmol) in 1 mL of CH_3CN. To the resulting dark blue solution was added 61 mg of tetrachlorocatechol ×hydrate (this is only necessary if crystalline product is desired; otherwise the complex precipitates out from the solution as a light blue powder). Upon diethyl ether diffusion into the dark green solution, dark blue crystals could be isolated from the solution after 12 h. They were dried under high vacuum, where they lost their coordinated CH_3CN. $CuC_{23}H_{30}N_4O_{15}Cl_2$ (736.96), calcd (found): C 37.49 (37.53), H 4.10 (4.39), N 7.60 (7.60). FAB^+-MS: 599 ($(M - ClO_4 - 1)^+$; 100%); 519 ($(Cu(L^1)\cdot H_2O)^+$; 70%). IR [cm^{-1}]: 1736 (s), 1612 (m), 1447 (m), 1268 (s), 1120, 1080 (vs), 778 (m).

Copper(II) Complexes of Me-L^1. These were prepared in a manner similarly to the corresponding copper(II) complexes of L^1 from Me-L^1 (50 mg) and copper(II) salt in 1 mL of CH_3CN. Diethyl ether diffusion into the CH_3CN solution led to blue (ClO_4^-) or turquoise (Cl^-) crystalline material.

$[Cu(Me\text{-}L^1)Cl]Cl\cdot 2H_2O$. $CuC_{25}H_{34}N_4O_7Cl_2$ (637.02), calcd (found): C 47.13 (47.80), H 5.34 (4.92), N 8.80 (8.93). FAB^+-MS: 547 ($[Cu(Me\text{-}L^1)]\cdot H_2O + 1$; 50%), 582 ($[Cu(Me\text{-}L^1)Cl]^+\cdot H_2O + 1$; 100%).

$[Cu(Me\text{-}L^1)](ClO_4)_2\cdot 2H_2O\cdot 0.5CH_3CN$: $CuC_{26}H_{35.5}N_{4.5}O_{15}Cl_2$ (785.5), calcd (found): C 39.72 (39.67), H 4.52 (4.66), N 8.02 (7.76).

Dicopper(II) Complexes of L^2. These were prepared in a manner similar to the copper(II) complexes with L^1 from L^2 (100 mg, 0.115 mmol) in CH_3CN (1 mL) and the corresponding copper(II) salt (0.23 mmol) in CH_3CN (1 mL).

$[Cu_2(L^2)Cl_2]Cl_2\cdot 5H_2O$. $Cu_2C_{46}H_{60}N_8O_{15}Cl_4$ (1233.93), calcd (found): C 44.78 (44.66), H 4.90 (4.88), N 9.08 (9.47). FAB^+-MS: 1107 ($[Cu_2(L^2)Cl_2]Cl^+$, 30%); 1072 ($[Cu_2(L^2)Cl_2]^+$; 50%); 1037 ($[Cu_2(L^2)Cl]^+$; 58%); 937 ($[Cu(L^2)]^+$; 50%).

$[Cu_2(L^2)](ClO_4)_4\cdot 4H_2O$. $Cu_2C_{46}H_{58}N_8O_{30}Cl_4$ (1471.91), calcd (found): C 37.54 (37.55), H 3.97 (3.93), N 7.61 (7.59).

Dicopper(II) Complexes of L^3. These were prepared in a manner similar to the copper(II) complexes with L^1 from L^3 (100 mg, 0.115 mmol) in CH_3CN (1 mL) and the corresponding copper(II) salt (0.23 mmol) in CH_3CN (1 mL).

$[Cu_2(L^3)Cl_2]Cl_2\cdot 5H_2O$. $Cu_2C_{47}H_{62}N_8O_{15}Cl_4$ (1247.96), calcd (found): C 45.24 (45.33), H 5.00 (5.00), N 8.97 (9.04). FAB^+-MS: 1157 ($(Cu_2(L^3)Cl_4)^+$, 18%), 1122 ($[Cu_2(L^3)Cl_3]^+$, 40%). IR [cm^{-1}]: 1734 (vs), 1616, 1607 (s), 1258 (s).

$[Cu_2(L^3)](ClO_4)_4\cdot 5H_2O$. $Cu_2C_{47}H_{62}N_8O_{31}Cl_4$ (1503.95), calcd (found): C 37.54 (37.40), H 4.16 (4.42), N 7.45 (7.28).

$[Cu_2(L^4)Cl_2]Cl_2\cdot 3H_2O$. $Cu_2C_{52}H_{60}N_8O_{13}Cl_4$, (1273.99) calcd (found): C 49.02 (49.17), H 4.71 (4.77), N 8.80 (8.87).

$[Cu_2(L^4)](BF_4)_4\cdot H_2O$. $Cu_2C_{52}H_{56}N_8O_{11}B_4F_{16}$, (1443.37) calcd (found): C 43.24 (43.18), H 3.88 (4.71), N 7.76 (7.76).

Crystal Structure Determinations. Crystal data and experimental details are given in Table 5. Diffraction data for $[Cu(L^3)(NCCH_3)_2](PF_6)$, $[Cu(L^2)(NCCH_3)_2](ClO_4)_4$, and $[Cu_2(L^3)(Cl)_2]Cl_2$ were collected on a Smart 1000 CCD diffractometer (Mo Kα radiation, $\lambda = 0.71073$ Å, ω scan) at −100 or −73 °C ($[Cu_2(L^3)Cl_2]Cl_2$), for $[Cu_2(L^{2'})(NCCH_3)_2](SbF_6)_2$ on a Siemens-Stoe four-circle diffractometer at −70 °C. Data were corrected for Lp and

absorption effects. The structures were solved by direct methods and refined by full-matrix least-squares methods on F^2.[68]

Acknowledgment. Financial support by the Deutsche Forschungsgemeinschaft (DFG) is gratefully acknowledged. H.B. is grateful for a fellowship from the LGF Baden-Wuerttemberg. S.S. is grateful to Prof. Rudi van Eldik for support.

(68) Sheldrick, G. M. *SHELXTL 5.1*; Bruker AXS: Madison, WI, 1998.
(69) Wei, N.; Lee, D.-H.; Murthy, N. N.; Tyeklar, Z.; Karlin, K. D.; Kaderli, S. *Inorg. Chem.* **1994**, *33*, 4625.
(70) Baldwin, M. J.; Ross, P. K.; Pate, J. E.; Tyeklar, Z.; Karlin, K. D.; Solomon, E. I. *J. Am. Chem. Soc.* **1991**, *113*, 8671.

Supporting Information Available: Complete information on all crystal structure studies. This material is available free of charge via the Internet at http://pubs.acs.org.

IC011114U